On the self assembly of short chain alkanedithiols

Hicham Hamoudi,[ab] Zhiang Guo,[c] Mirko Prato,[d] Céline Dablemont,[ab] Wan Quan Zheng,[c] Bernard Bourguignon,[c] Maurizio Canepa[d] and Vladimir A. Esaulov*[ab]

Received 9th June 2008, Accepted 22nd August 2008
First published as an Advance Article on the web 3rd October 2008
DOI: 10.1039/b809760g

A study of the self-assembly of nonane-alkanedithiol monolayers on gold in *n*-hexane and ethanol solvents is presented. Self-assembled monolayers (SAMs) are characterised by reflection–absorption infrared spectroscopy (RAIRS), sum frequency generation (SFG) and spectroscopic ellipsometry (SE) measurements. Data obtained for alkanethiols SAMs are also shown for comparison. The measurements show that nicely organized HSC_9SH SAMs can be obtained in *n*-hexane provided that N_2-degassed solutions are used and all preparation steps are performed in the absence of ambient light. SFG measurements show that these SAMs have free standing SH groups. Use of an un-degassed and/or light-exposed *n*-hexane solutions leads to a worse layer organization. Preparation in ethanol, even in degassed solutions with processing in the dark, leads to poorly organized layers and no sign of free –SH groups was observed.

Introduction

Formation of metallic nanostructures and/or metallic thin layers on organic structures is an important goal in the field of organic–inorganic hybrid materials for new electronic devices and sensors. For such polymer-based components, the quality of the metal/organic layer interface determines the efficiency and the longevity of the electronic element.[1] As a consequence, a good knowledge of the metal/organic interface is necessary, which is however difficult to reach in the case of polymers.[2] An alternative to the use of polymers relies on self-assembled monolayers (SAMs) of organic molecules on a metallic surface. Indeed, SAMs are attractive because they allow surface functionalization with desired chemical groups.[3–20] For instance, an alkanedithiol SAM functionalizes the support with thiol groups. The pending SH group allows grafting of metallic atoms or nanoparticles and further growth of metallic nanostructures or thin films. Our interest in dithiol SAMs stems specifically from this aspect and this work focuses on formation of alkanedithiol SAMs on gold supports.

Numerous reports on the preparation and application of dithiol SAMs are available in the literature. The SAMs have been characterised by different techniques including *e.g.* XPS, UPS, single wavelength ellipsometry, STM/AFM, SIMS, RAIRS, SFG, contact angle measurements, cyclic voltammetry *etc.*[21–40] Despite the relatively large amount of work done, the conditions for the reproducible formation of well ordered SAMs with free SH endgroups are still debated.[21,41–44]

It is well known that the formation of alkanethiol SAMs proceeds through two steps: first, formation of a so-called striped phase with the alkyl chains lying parallel to the gold support and then formation of the so-called standing up phase.[21,22] The case of dithiols is more complex as has been very recently discussed by Scoles and coworkers.[21] In the case of dithiols, formation of an initial phase with both mercapto groups bound to the surface may hinder the development of the standing-up phase. A major problem here could be the formation of mixed, lying down and standing up phases. The choice of the preparation method of the alkanedithiol SAM is therefore critical. In a solvent-free strategy, the alkanedithiol is evaporated directly onto the metal substrate under UHV conditions. In such a case a lying down phase was reported.[23] This situation may also occur for SAMs prepared from the liquid phase.[24,25]

Regarding preparation from solutions, different solvents can be utilized *e.g.* ethanol, *n*-hexane or toluene. It has been pointed out that alkanedithiols are sensitive to oxidation, especially in presence of ambient light, leading to formation of sulfonates or to disulfide bridges[26,27] and in some cases multilayers.[26] From available literature, *n*-hexane[26] which is less permeable to dioxygen than the commonly used ethanol,[28] and more solvating than toluene, seems to be the best choice. Photooxidation processes may also affect the stability of the prepared SAM in ambient conditions.[29,30]

In some cases more complex procedures have been used where good quality SAMs have been achieved using aromatic dithiols resorting to endgroup capping in an intermediate step or in some cases employing mixed endgroup molecules.[41,42]

Given the interest in the use of dithiol SAMs in various applications, in this work we addressed the assembly of a nonanedithiol SAMs from solution onto gold substrates, in an attempt to establish a reproducible protocol for obtaining good quality SAMs. An experimental approach is adopted, which combines three "gentle" methods able to offer insight into several complementary aspects. Spectroscopic ellipsometry

[a] *Université-Paris Sud, Laboratoire des Collisions Atomiques et Moléculaires, LCAM, Bâtiment, 351, UPS-11, 91405 Orsay, France. E-mail: vladimir.esaulov@u-psud.fr*
[b] *CNRS, UMR 8625, Laboratoire des Collisions Atomiques et Moléculaires, LCAM, Bâtiment, 351, UPS-11, 91405 Orsay, France*
[c] *CNRS, UPR 3361, Laboratoire de Photophysique Moléculaire, LPPM, Bâtiment, 350, UPS-11, 91405 Orsay, France*
[d] *CNISM and Department of Physics, University of Genova, Via Dodecaneso, 33, 16146 Genova, Italy*

(SE) is used to characterise the UV-VIS properties of the substrates and of the interface. Further, it can be effectively employed to get estimates of the thickness of the deposited layers, obtaining a first insight on the SAM organization and quality. RAIRS and SFG are employed to provide specific spectroscopic fingerprints on the SAM organization.

SFG provides information in a restricted spectral range with respect to RAIRS, but it is more strongly dependent on order and symmetry, and may allow detection of the endgroup with higher sensitivity. Reproducibly well organised dithiol SAMs were obtained for tens of experiments, when during incubation the *n*-hexane solution is carefully degassed and light exposure is avoided.

The strategy used to obtain well ordered SAMs from a *n*-hexane solution is described along with aspects of SAM stability and response to light.

Experimental

SAM preparation

In order to get well-organized SAMs, the quality of the gold surface is a key parameter. In the literature several types of supports have been used, ranging from polycrystalline gold, to Au(111) single crystal[23,27] and to vacuum gold evaporation onto various supports such as freshly cleaved mica sheets,[22,24,25,31–36] glass[29–31,37] and silicon wafers.[26,38–40] In all cases one obtains large flat Au(111) terraces. Here we used commercial (Arrandee) gold on glass substrates.

The gold substrates were made of 0.7 mm thick borosilicate glass, covered by a 2.5 nm thick chromium adhesion layer and by a 250 nm thick final gold layer. For this work, the substrates were annealed thrice in a butane/propane flame for 2 min, with intermediate coolings performed under a N_2 flow. Final rinsing was done with absolute ethanol before drying under N_2. HSC_9SH 97% from Alfa Aesar, 1-hexanethiol 95% (C_6SH) from Fluka, 1-dodecanethiol 98% ($C_{12}SH$), 1-pentadecanethiol 98% ($C_{15}SH$), from Aldrich and *n*-hexane 99% from Riedel-de Haën were used without further purification.

The flame annealed substrates were checked by SE just prior to the incubation in the solution. The dielectric function derived from SE on flame annealed gold gave results in excellent agreement with benchmark literature.[45]

Alkanethiol SAMs were prepared by immersing the gold support into a freshly prepared 1 mM solution of C_nSH in ethanol for times ranging from 30 min to 24 hours at room temperature.

In the case of alkanedithiols different procedures were adopted. The SAMs were prepared in ethanol and in *n*-hexane. The SAMs were prepared by immersion into a 1 mM solution in ethanol for 24 hours, while for *n*-hexane samples were placed in a 1 mM solution for about 1 hour. We used solutions freshly degassed by N_2 bubbling.

The samples were then rinsed with the same (fresh) solvent of the solution, and dried with N_2.

The effect of ambient light during immersion, rinsing and measurements was investigated.

Infrared spectroscopy

The FT-IR spectrometer used for analysis is a Bruker Vertex 70. It can be equipped either with a demountable gas cell with ZnSe windows for transmission spectra or with a home made reflection attachment for RAIRS measurements. In this case the incident angle was 80° to the surface normal. A deuterated triglycine sulfate (DTGS) detector was used to detect either the transmitted or the reflected light. Some reference spectra of gas phase thiols and dithiols were taken with the spectral resolution set at 1 cm^{-1}. For the SAM measurements, the spectral resolution was set to 4 cm^{-1}. The spectrometer and sample are flushed first with dry air and during measurements by a N_2 flow.

Sum frequency generation (SFG)

The broad band SFG set-up[46] is detailed elsewhere.[47–49] Tunable IR pulses (4 μJ, 145 fs, 150 cm^{-1} bandwidth) and "visible" pulses (800 nm, 2 μJ, Fourier limited duration corresponding to an adjustable bandwidth of a few cm^{-1}) are superimposed on the sample in a collinear, co-propagating configuration at an incident angle of 60° in p-polarization. The reflected SFG signal is detected after a monochromator on a cooled CCD camera. The monochromator resolution can be as high as one single pixel (0.4 cm^{-1} at 650 nm). The spectrum resolution is limited by the visible beam bandwidth, which is decreased until the spectrum does not change. The broadband SFG response of the molecules interferes with the non resonant response originating from the Au surface. The latter has the spectral shape of the femtosecond IR laser. The spectral profile of the IR laser is experimentally obtained by measuring the non resonant response that arises from a GaAs reference sample. In what follows we present either the difference signal between the non resonant and the vibrational responses, or the deconvolution in individual vibrational bands. The fitting procedure was described in ref. 47.

Spectroscopic ellipsometry (SE)

Principles of UV-SE are described at length in books[50,51] and reviews.[52] Specific application to SAMs is addressed in details in ref. 45.

In brief, the output of standard ellipsometry measurements is the reflection coefficient $\rho = r_p/r_s = \tan \Psi \exp(i\Delta)$ where r_p and r_s are the complex Fresnel reflection coefficients for p- and s-polarization, respectively. The phase angle Δ ensures enhanced sensitivity to the presence of ultra thin films.[50]

Under the Fresnel scheme, the system under investigation is usually conceived as a stack of layers on a substrate. In the crudest approach the layers are separated by sharp interfaces. The optical complex function N_j ($n_j(\lambda)$, $k_j(\lambda)$) and the effective thickness d_j of each layer are used as free parameters in fitting routines.[51]

The rotating compensator spectroscopic ellipsometer, (M-2000, J.A. Woollam Co. Inc.) allows simultaneous measurements at 225 different wavelengths in the range 245–725 nm. It was tested and used in several works on thin and ultrathin layers.[45,53,54]

The experimental protocol adopted for SE measurements on ultrathin layers has been thoroughly described in a recent

article on thiolate SAMs on gold.[45] Spectra have been collected at two angles of incidence, 65 and 70 degrees. The spot size on the sample was of the order of a few mm^2.

Results and discussion

Alkanedithiol SAM from an *n*-hexane solution

SE measurements performed on HSC_9SH SAMs grown in *n*-hexane (dark vertical bar, average over 10 samples) and in ethanol (light vertical bar, average over 5 samples) are shown in Fig. 1. The solutions were thoroughly degassed and kept in the dark. Data are shown as difference spectra between the film-covered samples and substrates ($\delta\Psi = \Psi_{film} - \Psi_{Au}$, $\delta\Delta = \Delta_{film} - \Delta_{Au}$), in order to emphasize the fine changes induced by the formation of nanometer thick layers. In Fig. 1, the experimental data obtained for dithiols are compared with those obtained for $C_{12}SH$ SAMs. The small vertical error bars in the high-wavelength region are useful to visualize the distribution of the data related to sample-to-sample variations.

The overall shape of $\delta\Psi$ and $\delta\Delta$ spectra resembles closely the data obtained on alkanethiols SAMs.[45] In particular, the $\delta\Psi$ curves exhibit the typical transition from positive to negative values in correspondence with the $\delta\Delta$ maxima, already observed for other thiolate interfaces.[45] $\delta\Delta$ patterns related to samples grown in *n*-hexane show values close to those observed on $C_{12}SH$ SAMs.

Dashed lines in Fig. 1. represent the results of a few indicative simulations obtained using a four-phase model (ambient/transparent layer/interface/substrate). The optical model and the effective thickness (0.35 nm) of the S–Au interface were optimized in reference 45 on $C_{18}SH$ SAMs.

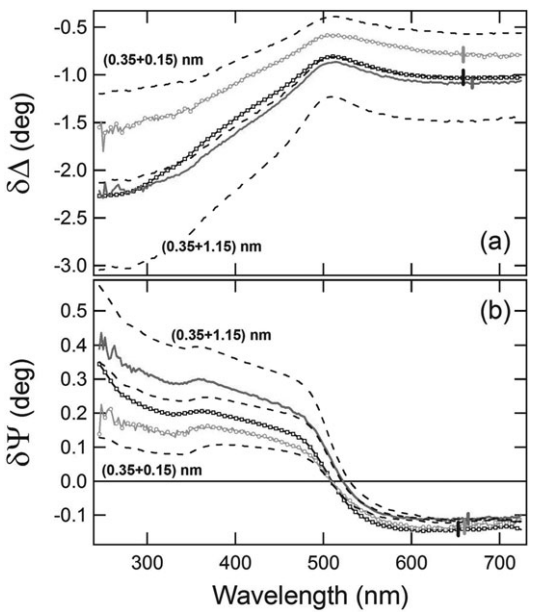

Fig. 1 SE measurements performed on HSC_9SH SAMs grown in *n*-hexane (dark vertical bar and circles) and in ethanol (light vertical bar and squares). Data for $C_{12}SH$ SAMs are shown for comparison (full line). Dashed lines represent the results of simulations for total film thickness of 0.5, 1.0 and 1.5 nm (see text).

The refraction index of the transparent layer was kept fixed at 1.475, a reasonable value for packed alkyl chains.[45] The simulations represent the spectral variations induced by films of total thickness (interface + chains) of 0.5, 1.0 and 1.5 nm.

Taking also in account the simulations, the ellipsometric thickness of HSC_9SH film grown in *n*-hexane turns out to be of the order of 1 nm. This value is compatible with a rather compact standing-up phase SAM with tilted molecules.

A closer comparison between the patterns of dithiol SAMs grown in *n*-hexane and $C_{12}SH$ SAMs shows some subtle shape difference, visible in particular in the $\delta\Delta$ curve in the low-wavelengths range (below 300 nm). Those differences may be indicative of weak optical absorptions specific of dithiol layers, with bridging S–S bonds. Absorptions related to the presence of S–S bonds are indeed expected in the 250–330 nm region.[55] The S–S bonding is thought to arise from the SAM/air interface rather than from the Au/SAM interface as discussed by others authors.[27,55]

RAIRS spectra on dithiol SAMs grown in degassed *n*-hexane and with all processing done in the dark are shown in Fig. 2 (a and b) and display a peak corresponding to $\upsilon_{as}(CH_2)$ at 2918 cm^{-1}. We also observe a peak at 2850 cm^{-1} for the symmetric stretch $\upsilon_s(CH_2)$. This finding is in agreement with the value of 2919 cm^{-1} found by Blanchard *et al.*[26] for a HSC_9SH SAM also prepared in degassed *n*-hexane, though lighting conditions were not indicated.

For the interpretation of these values it is useful to compare the measurements with reference data obtained on alkanethiols. RAIRS spectra obtained for some well-organized alkanethiol SAMs on gold, prepared from an ethanol solution, are shown in Fig. 3. We observe a peak corresponding to $\upsilon_{as}(CH_2)$ located around 2917 cm^{-1} for long chain alkanethiols and 2921 cm^{-1} for the ones with short chain in agreement with literature.[3] Indeed, $\upsilon_{as}(CH_2)$ peak is red-shifted of at least 5 cm^{-1} with respect to the gas phase value. We also observe 2850 cm^{-1} for the symmetric stretch $\upsilon_s(CH_2)$. The ratio $\upsilon_{as}(CH_3)/\upsilon_s(CH_3)$ is more important for chains with even number of CH_2 groups (case of $C_{15}SH$) because of RAIRS sensitivity to dipolar moment interaction with the surface. The structures at 2879 cm^{-1}, 2964 cm^{-1} and the shoulder at 2935 cm^{-1} correspond respectively to symmetric, and antisymmetric CH_3 vibrations and a Fermi resonance.

With regard to –SH vibrations, transmission spectra of alkanethiols and dithiols (Fig. 4) in the gas phase provide useful reference spectra. We recorded the spectra for C_6SH and HSC_5SH which possess the same number of methylene units. The SH peak located at 2565 cm^{-1} is more intense for HSC_5SH than for C_6SH, because of the two SH groups. However, it remains weak by comparison to the CH vibration signals, which, in the gas phase, appears at 2927 cm^{-1} for the antisymmetric vibration $\upsilon_{as}(CH_2)$ and 2854 cm^{-1} for the symmetric stretch $\upsilon_s(CH_2)$. In the case of spectra recorded for HSC_9SH, the SH peak is weaker than for HSC_5SH when compared to the CH peaks.

The RAIRS 2918 cm^{-1} value is therefore fully consistent with a well organized HSC_9SH SAM on gold. In our case, the $\upsilon_{as}(CH_2)$ signal intensity is of the same order of magnitude as the one obtained with 1-dodecanethiol ($C_{12}SH$), which is also consistent with SE data and indicates functionalization with a

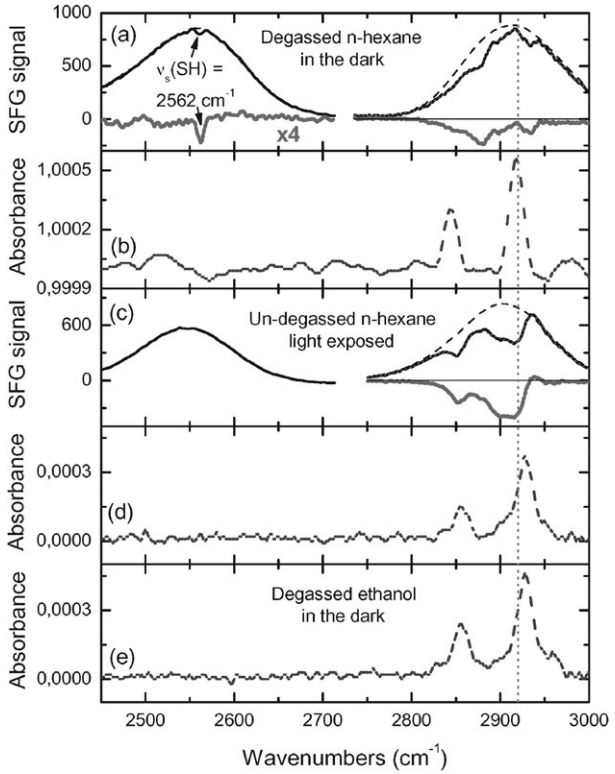

Fig. 2 RAIRS and SFG spectra of organized (a and b) and disorganized (c, d and e) HSC_9SH SAMs on gold substrate. Experimental SFG reference spectrum (dashed line), experimental SFG spectrum (solid bold line), result of the subtraction between experimental SFG reference spectrum and experimental SFG spectrum (tight dashed bold line) of HSC_9SH on gold substrate (see line legends in insert of Fig. 3). For the spectra a and b, the SAM has been grown in degassed *n*-hexane in the dark and is organised (in SFG SH is detectable, CH_2 is absent. In RAIRS the CH_2 asymmetric stretch frequency is "low"). For the spectra c and d, the SAM has been synthesized in undegassed *n*-hexane, exposed to the light and is disorganised (CH_2 is present in SFG, SH is absent, the frequency of CH_2 asymmetric stretch has shifted to the blue). The spectrum e has been obtained in degassed ethanol in the dark and is disorganised. The dotted vertical line indicates the position of 2920 cm^{-1}, which corresponds to the $\nu_{as}(CH_2)$ vibration in an organised SAM.

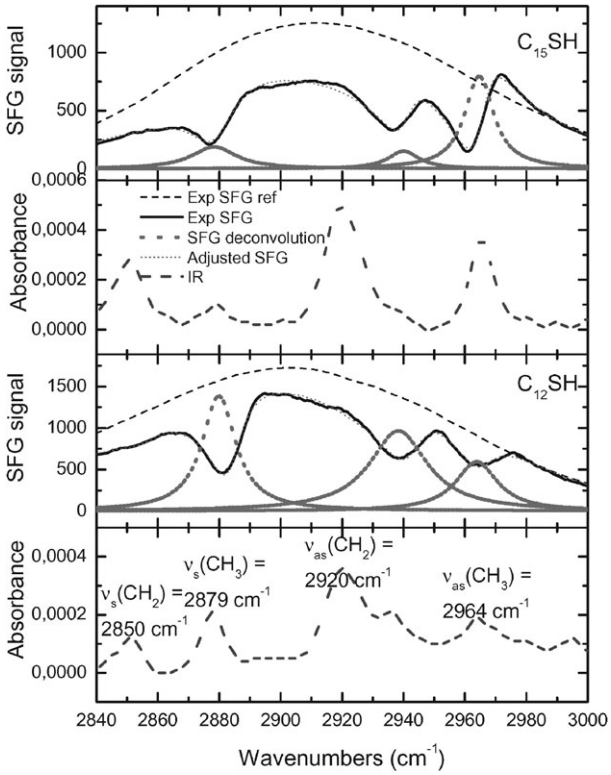

Fig. 3 RAIRS and SFG spectra of $C_{12}SH$ and $C_{15}SH$. Experimental SFG reference spectrum (dashed line), experimental SFG spectrum (solid bold line), SFG deconvolution (tight dashed bold line), adjusted SFG spectrum (dotted line) and IR spectrum (scattered dashed bold line) of $C_{12}SH$ (bottom) and $C_{15}SH$ (top) SAMs organised on gold support. The SAMs are well organised: only the CH_3 bands are present in SFG. The intensities depend on the orientation of CH_3, which varies with the parity of the chain length. The same orientation effect is also manifest in the CH_3 RAIRS intensities.

monolayer thick ordered film. In the RAIRS spectra we do not observe any signal at 2565 cm^{-1} specific of free SH, which is consistent with the weak signal observed in the gas phase. Concerning the reproducibility of RAIRS measurements we note that we did observe some scatter in the position of this $\upsilon_{as}(CH_2)$ peak in the multiple RAIRS measurements performed on various samples, in which the $\upsilon_{as}(CH_2)$ peak appeared in the 2918–2921 cm^{-1} range.

The good organization of our HSC_9SH SAM on gold is confirmed by the SFG data also presented in Fig. 2. It is convenient to compare the data with spectra obtained on alkanethiols which are also shown for comparison in Fig. 3.

Absence of SFG signal for CH_2 is characteristic of alkanethiol organization on the surface (Fig. 3). In the literature it is usually explained by the fact that contributions of CH_2 in a centrosymmetric relation is equal to zero. This is the case in the all-*trans* conformation. It was shown that in the case of an

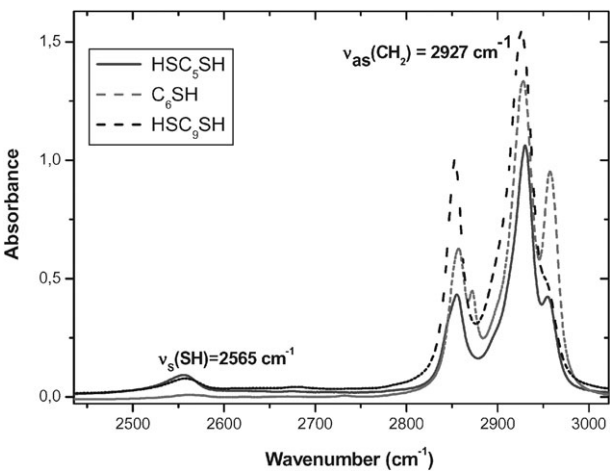

Fig. 4 FT-IR transmission spectra of C_6SH (dashed line), HSC_5SH (solid line) and HSC_9SH (dotted line) in the gas phase.

odd number of CH_2 groups the orientation of the unpaired CH_2 with respect to the surface plane must also be invoked, and gauche defects at the bottom of the chain with an appropriate orientation may also be compatible with the

absence of CH_2 in the SFG spectrum.[56] However the absence of the CH_2 bands is nevertheless characteristic of an ordered SAM, most of the chain being all-trans. In the cases of $C_{18}SH$ and $C_{12}SH$ SFG spectra are very similar as they only present CH_3 bands and as CH_3 groups are oriented in the same way in both molecules: in an all-trans chain, removing an even number of CH_2 does not change the CH_3 orientation. The important difference seen on RAIRS between chains with even or odd number of CH_2 is also observed in SFG. It is qualitatively understandable by the alternative orientation of CC bonds in an all-trans alkyl chain: removing an odd number of CH_2 changes the CH_3 orientation. A quantitative analysis of these spectra is presented elsewhere.[57]

The absence of signal for the methylene unit in the SFG spectrum (Fig. 2) confirms the good organization of our HSC_9SH SAM on gold. In the region of the υ(CH) bands, the only signals visible on the SFG spectrum are CH_3 peaks, which are attributed to traces of solvent not visible in the RAIRS spectrum because of their very weak intensity. An important new feature observed on the SFG spectrum is the dip located at 2562 cm^{-1}, a frequency corresponding to free S–H. To our knowledge, its observation by SFG was not reported before. It is difficult to observe, due to both its intensity which is close to the detection limit and the fact that it decays with time. Its weak intensity is not unexpected considering that the absorbance of SH in the gas phase is 14 times smaller than that of the methyl bands (Fig. 4). Its decay with time is in contrast to the case of methyl bands which are observed to be stable for months in the SAMs of alkanethiols. We attribute it to photoinduced oxidation, since recording SFG spectra implies exposure of the molecules to visible laser light under ambient conditions.

Summarising our SFG results, well organised SAMs of HSC_9SH could be reproducibly formed in *n*-hexane, with observable free SH end group. It should be stressed here that this could only be obtained in the case of the best samples prepared with degassed solutions and when all the preparation procedure was carried out in the absence of ambient light. Preparation in un-degassed solutions and/or in conditions of ambient light would systematically yield 2927 cm^{-1} for the antisymmetric vibration $\upsilon_{as}(CH_2)$ and 2854 cm^{-1} for the symmetric stretch $\upsilon_s(CH_2)$.

No clear spectral evidence of the formation of S–S bridges at the SAM-air interface was obtained. In particular RAIRS spectra did not show the weak 500 cm^{-1} peak due to S–S stretching. The existence of S–S bonds has been discussed by some authors[29] although in their and some other XPS studies the peak at about 164 eV attributable to free SH, would be difficult to distinguish from a disulfide contribution. The existence of disulfide has however been reported in HREELS measurements[58] with the SAM prepared in an aqueous solution with 0.5 M KOH used for electrochemistry.

Alkanedithiol SAM from an ethanol solution

SE measurements on HSC_9SH SAMs grown in ethanol (Fig. 1) indicate that the layers are apparently less thick than in the *n*-hexane case, probably indicating a less compact, more disordered layer. In our experiments we did not observe formation of multilayers.

Fig. 2 (e) shows the RAIRS spectrum for HSC_9SH prepared in ethanol. The overall intensity of the CH_2 peaks appeared to be of the order of the ones observed for dodecanethiol (Fig. 3, bottom) suggesting that we are dealing with a monolayer, a conclusion that would agree with the SE measurements. The antisymmetric vibration $\upsilon_{as}(CH_2)$ appears at around 2927 cm^{-1} and around 2854 cm^{-1} for the symmetric stretch $\upsilon_s(CH_2)$. As mentioned above these values are characteristic of a disorganized alkyl chain. As in the case of *n*-hexane, the SH peak located at 2565 cm^{-1} was not visible in RAIRS spectra, and we also did not observe it in SFG. The SFG spectrum also clearly indicated a significant loss of order with respect to *n*-hexane. The methylene bands are strong, which reveals the presence of CH_2 groups oriented significantly out of the surface plane and a not all-*trans* configuration.

Attempts at degassing the ethanol solution with N_2 to minimise dissolved dioxygen and performing all the work in dark conditions yielded similarly unsatisfactory results. In RAIRS the antisymmetric vibration $\upsilon_{as}(CH_2)$ systematically appears at around 2927 cm^{-1} and around 2854 cm^{-1} for the symmetric stretch $\upsilon_s(CH_2)$. We would conclude here that in the ethanol solution we obtained a SAM of standing up molecules as shown by SE, but the organisation was poor compared to the one obtained in a reproducible manner in *n*-hexane. Our observations in ethanol could be compatible with the formation of disulfide bridges on top of the SAM, leading to distortions of the molecules as suggested by some recent calculations,[27] and to the modifications of the RAIRS and SFG spectra, showing some disorganisation.

The overall poor organisation of the dithiol SAM in ethanol is in agreement with the conclusions of a very recent STM study.[21] The data therefore show that organization of nonanedithiol monolayers depends on the nature of the solvent. Besides questions related to traces of *e.g.* dissolved oxygen, an influence of solvation properties on the adsorption process could be envisaged. The best solvent could favour the ordering process both affecting the adsorption dynamics and decreasing the probability of forming phases with both mercapto groups bound to the surface. One could also question the role of the presence of the smaller ethanol solvent molecules in the SAM and their influence on endgroup reactions.

Conclusions

We have presented a study of alkanedithiol SAMs on gold and compared it with that of some alkanethiols. SE, RAIRS and SFG show that well organized nonanedithiol SAMs, about 1 nm thick, can be obtained in degassed *n*-hexane solutions with all the preparation procedure performed in the absence of ambient light. SFG shows that the SAMs have free standing SH groups.

RAIRS and SFG show that SAMs formed in ethanol are not well organised. SE shows that in this case the thickness of the SAM is somewhat smaller than for the one prepared in degassed *n*-hexane, but would appear to be compatible with standing up molecules.

The effect of ambient light and laser intensity on the SAM was noted indicating instability probably related to photooxidation of the free SH groups.

The procedure of dithiol SAM preparation could thus be useful in applications involving growth of metallic films and nanoparticles, as in molecular electronics.

References

1 M. Fahlman and W. R. Salaneck, *Surf. Sci.*, 2002, **500**, 904–922.
2 T. Strunskus, V. Zaporojtchenko, K. Behnke, C. von Bechtolsheim and F. Faupel, *Adv. Eng. Mater.*, 2000, **2**, 489–492.
3 M. D. Porter, T. B. Bright, D. L. Allara and C. E. D. Chidsey, *J. Am. Chem. Soc.*, 1987, **109**, 3559–3568.
4 R. G. Nuzzo, F. A. Fusco and D. L. Allara, *J. Am. Chem. Soc.*, 1987, **109**, 2358–2368.
5 R. G. Nuzzo, L. H. Dubois and D. L. Allara, *J. Am. Chem. Soc.*, 1990, **112**, 558–569.
6 P. E. Laibinis, G. M. Whitesides, D. L. Allara, Y.-T. Tao, A. N. Parikh and R. G. Nuzzo, *J. Am. Chem. Soc.*, 1991, **113**, 7152–7167.
7 A. Hooper, G. L. Fisher, K. Konstadinidis, D. Jung, H. Nguyen, R. Opila, R. W. Collins, N. Winograd and D. L. Allara, *J. Am. Chem. Soc.*, 1999, **121**, 8052–8064.
8 K. Heister, D. L. Allara, K. Bahnck, S. Frey, M. Zharnikov and M. Grunze, *Langmuir*, 1999, **15**, 5440–5443.
9 G. L. Fisher, A. E. Hooper, R. L. Opila, D. L. Allara and N. Winograd, *J. Phys. Chem. B*, 2000, **104**, 3267–3273.
10 A. V. Walker, T. B. Tighe, O. M. Cabarcos, M. D. Reinard, B. C. Haynie, S. Uppili, N. Winograd and D. L. Allara, *J. Am. Chem. Soc.*, 2004, **126**, 3954–3963.
11 C. D. Bain, E. B. Troughton, Y.-T. Tao, J. Evall, G. M. Whitesides and R. G. Nuzzo, *J. Am. Chem. Soc.*, 1989, **111**, 321–335.
12 J. C. Love, L. A. Estroff, J. K. Kriebel, R. G. Nuzzo and G. M. Whitesides, *Chem. Rev.*, 2005, **105**, 1103–1169.
13 N. Camillone, C. E. D. Chidsey, G. Y. Liu, T. M. Putvinski and G. Scoles, *J. Chem. Phys.*, 1991, **94**, 8493–8502.
14 N. Camillone, C. E. D. Chidsey, G. Y. Liu and G. Scoles, *J. Chem. Phys.*, 1993, **98**, 3503–3511.
15 M. F. Danisman, L. Casalis, G. Bracco and G. Scoles, *J. Phys. Chem. B*, 2002, **106**, 11771–11777.
16 F. Teran Arce, M. E. Vela, R. C. Salvarezza and A. J. Arvia, *Langmuir*, 1998, **14**, 7203–7212.
17 C. Vericat, M. E. Vela and R. C. Salvarezza, *Phys. Chem. Chem. Phys.*, 2005, **7**, 3258–3268.
18 G. E. Poirier, *Chem. Rev.*, 1997, **97**, 1117–1127.
19 F. Schreiber, *Prog. Surf. Sci.*, 2000, **65**, 151–256.
20 S. M. Barlow and R. Raval, *Surf. Sci. Rep.*, 2003, **50**, 201–341.
21 J. Liang, L. G. Rosa and G. Scoles, *J. Phys. Chem. C*, 2007, **111**, 17275–17284.
22 K. Kobayashi, H. Yamada, T. Horiuchi and K. Matsushige, *Appl. Surf. Sci.*, 1999, **144–145**, 435–438.
23 T. Y. B. Leung, M. C. Gerstenberg, D. J. Lavrich, G. Scoles, F. Schreiber and G. E. Poirier, *Langmuir*, 2000, **16**, 549–561.
24 K. Kobayashi, T. Horiuchi, H. Yamada and K. Matsushige, *Thin Solid Films*, 1998, **331**, 210–215.
25 K. Kobayashi, J. Umemura, T. Horiuchi, H. Yamada and K. Matsushige, *Jpn. J. Appl. Phys.*, 1998, **37**, L297–L299.
26 P. Kohli, K. K. Taylor, J. J. Harris and G. J. Blanchard, *J. Am. Chem. Soc.*, 1998, **120**, 11962–11968.
27 M. L. Carot, M. J. Esplandiu, F. P. Cometto, E. M. Patrito and V. A. Macagno, *J. Electroanal. Chem.*, 2005, **579**, 13–23.
28 J. Käshammer, P. Wohlfart, J. Weiβ, C. Winter, R. Fisher and S. Mittler-Neher, *Opt. Mater.*, 1998, **9**, 406–410.
29 M. J. Esplandiu, M. L. Carot, F. P. Cometto, V. A. Macagno and E. M. Patrito, *Surf. Sci.*, 2006, **600**, 155–172.
30 H. Rieley, G. K. Kendall, F. W. Zemicael, T. L. Smith and S. Yang, *Langmuir*, 1998, **14**, 5147–5153.
31 M. J. Esplandiu and P.-L. M. Noeske, *Appl. Surf. Sci.*, 2002, **199**, 166–182.
32 T. Ohgi, H.-Y. Sheng and H. Nejoh, *Appl. Surf. Sci.*, 1998, **130–132**, 919–924.
33 K. Vijaya Sarathy, P. John Thomas, G. U. Kulkarni and C. N. R. Rao, *J. Phys. Chem. B*, 1999, **103**, 399–401.
34 A. K. A. Aliganda, A.-S. Duwez and S. Mittler, *Org. Electron.*, 2006, **7**, 337–350.
35 A. K. A. Aliganda, I. Lieberwirth, G. Glasser, A.-S. Duwez, Y. Sun and S. Mittler, *Org. Electron.*, 2007, **8**, 161–174.
36 Y. Sakotsubo, T. Ohgi, D. Fujita and Y. Ootuka, *Phys. E*, 2005, **29**, 601–605.
37 S. Pethkar, M. Aslam, I. S. Mulla, P. Ganeshan and K. Vijayamohanan, *J. Mater. Chem.*, 2001, **11**, 1710–1714.
38 A.-S. Duwez, G. Pfister-Guillouzo, J. Delhalle and J. Riga, *J. Phys. Chem. B*, 2000, **104**, 9029–9037.
39 C. Winter, U. Weckenmann, R. A. Fisher, J. Käshammer, V. Scheumann and S. Mittler, *Chem. Vap. Deposition*, 2000, **6**, 199–205.
40 W. Deng, D. Fujita, L. Yang, H. Nejo and C. Bai, *Jpn. J. Appl. Phys.*, 2000, **39**, L751–L754.
41 Y. Tai, A. Shaporenko, H.-T. Rong, M. Buck, W. Eck, M. Grunze and M. Zharnikov, *J. Phys. Chem. B*, 2004, **108**, 16806–16810.
42 A. Niklewski, W. Azzam, T. Strunskus, R. A. Fischer and C. Wöll, *Langmuir*, 2004, **20**, 8620–8624.
43 Y.-C. Yang, Y.-L. Lee, L.-Y. Ou Yang and S.-L. Yau, *Langmuir*, 2006, **22**, 5189–5195.
44 L. Pasquali, F. Terzi, C. Zanardi, L. Pigani, R. Seeber, G. Paolicelli, S. M. Suturin, N. Mahne and S. Nannarone, *Surf. Sci.*, 2007, **601**, 1419–1427.
45 M. Prato, R. Moroni, F. Bisio, R. Rolandi, L. Mattera, O. Cavalleri and M. Canepa, *J. Phys. Chem. C*, 2008, **112**, 3899–3906.
46 L. J. Richter, T. P. Petralli-Mallow and J. C. Stephenson, *Opt. Lett.*, 1998, **23**, 1594–1596.
47 H. L. Zhang, S. D. Evans, K. Critchley, H. Fukushima, T. Tamaki, F. Fournier, W. Q. Zheng, S. Carrez, H. Dubost and B. Bourguignon, *J. Chem. Phys.*, 2005, **122**, 224707.
48 F. Fournier, W. Q. Zheng, S. Carrez, H. Dubost and B. Bourguignon, *Phys. Rev. Lett.*, 2004, **92**, 216102.
49 F. Fournier, W. Q. Zheng, S. Carrez, H. Dubost and B. Bourguignon, *J. Chem. Phys.*, 2004, **121**, 4839–4847.
50 R. M. A. Azzam and N. M. Bashara, in *Ellipsometry and Polarized Light*, North Holland, 1987.
51 H. Tompkins and E. Irene, in *Handbook of Ellipsometry*, NoyesData Corporation/Noyes Publications, 2005.
52 J. A. Woollam, B. Johs, C. M. Herzinger, J. N. Hilfiker, R. Synowicki and C. Bungay, *Proc. SPIE*, 1999, **CR72**, 1.
53 G. Gonella, O. Cavalleri, I. Emilianov, L. Mattera, M. Canepa and R. Rolandi, *Mater. Sci. Eng., C*, 2002, **22**, 359–366.
54 F. Bordi, M. Prato, O. Cavalleri, C. Cametti, M. Canepa and A. Gliozzi, *J. Phys. Chem. B*, 2004, **108**, 20263–20272.
55 W. Hoppe, W. Lohmann, H. Markl and H. Ziegler, in *Biophysics*, Springer, Berlin, 1983.
56 B. Bourguignon, W. Zheng, S. Carrez, F. Fournier and H. Dubost, *Chem. Phys. Lett.*, submitted.
57 Z. Guo, W. Zheng, H. Hamoudi, C. Dablemont, V. A. Esaulov and B. Bourguignon, *Surf. Sci.*, DOI: 10.1016/j.susc.2008.09.029.
58 S. Rifai, G. P. Lopinski, T. Ward, D. D. M. Wayner and M. Morin, *Langmuir*, 2003, **19**, 8916–8921.